Edinburgh Research Explorer

Operating Cycle Performance, Lost Periodicity and Waveform Distortion of Switch-Mode Power Supplies

Operating Cycle Performance, Lost Periodicity and Waveform Distortion of Switch-Mode Power Supplies

Xiao Xu , *Student Member, IEEE*, Adam. J. Collin, *Member, IEEE*, Sasa Z. Djokic, *Senior Member, IEEE*, Roberto Langella, *Senior Member, IEEE*, and Alfredo Testa, *Fellow, IEEE*

Abstract—**This paper investigates the performance of switch-mode power supplies used in desktop PCs (PC-SMPS') across the entire range of operating powers. Experimental results show that at low to medium operating powers, the input ac current might lose its periodicity with supply voltage frequency, when PCS-MPS' can be an unexpected source of interharmonics and dc component. In such cases, there is a significant increase of PC-SMPS' current waveform distortion and a substantial decrease of efficiency and operational power factors, which requires application of appropriate measurement and calculation procedures during the analysis. To correctly assess these power-dependent changes in performance and power quality indicators, the paper introduces a novel testing and evaluation methodology, based on the known or assumed PC-SMPS operating cycle.**

Index terms—**DC current; efficiency; harmonics; interharmonics; lost periodicity; operating cycle, power quality; switch-mode power supply.**

I. INTRODUCTION

SWITCH-MODE power supplies used in standard desktop PCs (PC-SMPS') are one of the most common types of power electronic (PE) equipment in the residential and commercial load sectors. For example, the percentage of the households with desktop PCs in the UK increased from ~13–85 % between 1985 and 2014, while the percentage of the population using computers on a daily basis increased from ~45% in 2006 to ~72% in 2015 [1-2]. The continuously increasing number of PC-SMPS' requires both close evaluation of their performance (e.g. efficiency) and assessment of their effects and impact on the network (e.g. harmonic emission). In this context, there is currently great interest at the international level in developing comprehensive and standardized testing procedures for evaluating the performance of PE equipment.

The development of new performance evaluation methods requires to carefully consider existing testing recommendations and to ensure compliance with widely utilized measurement procedures, e.g. in [3]. Current recommendations generally suggest multiple test points, as the device performance may vary with operating power [4, 5]. The two main PC-SMPS

efficiency certifications stipulate evaluation at four discrete operating powers (10, 20, 50 and 100 % of rated power, P_{rated}) [6-7], while [8] considers three discrete values (20, 50 and 100 % of P_{rated}). In contrast, power factor regulations [8] and harmonic emission [9] consider only P_{rated}. Besides the obvious discrepancies in the suggested test points, none of related legislation considers the actual times spent at different operating powers, i.e. the PC-SMPS operating cycle.

For assessing the performance of PV inverters, [10-11] suggest using a "weighted efficiency", based on predetermined times of operation at a few discrete power outputs. However, this is not considered in the PC-SMPS guidelines mentioned above and may be of particular importance in terms of the efforts aimed at reducing energy consumption in stand-by and low-power modes. For example, [8] evaluates PC-SMPS energy efficiency considering 'off', 'sleep' and 'idle' modes, which generally correspond to less than 10 % of P_{rated} [12], where a substantial deterioration of performance is observed for PC-SMPS' and other PE devices [4, 5, 13-15]. At these operating powers, the input ac current may lose periodicity with the supply voltage, which opens an important question of selecting appropriate measurement and calculation procedures. Although several methods have been proposed for calculating power quality (PQ) indices for non-stationary and aperiodic waveforms, e.g. [16-18], they are not always compatible with the framework in [3].

To correctly assess the power-dependent changes in the overall operational and PQ performance of PC-SMPS', this paper presents a novel testing and evaluation methodology, which considers the entire operating cycle of PC-SMPS. The developed measurement framework builds on the previous work in [15] by quantifying uncertainties in the test set-up and their impact on the obtained results and by providing further test results and a more detailed analysis of the operational and PQ performance of the tested PC-SMPS'. These results are then combined with the operating cycle data, to illustrate the methodology and its application, demonstrating that it is compatible with both the PMF and PDF operating cycle representations. Accordingly, the presented methodology can be applied for the analysis of other types of PE devices that operate with variable powers and under different operating cycles. The measurement procedures are developed to comply with the standard evaluation framework in [3], ensuring that the presented methodology can be easily applied to any PE equipment and any performance or PQ indicator.

X. Xiao and S. Z. Djokic are with the School of Engineering, the University of Edinburgh, Edinburgh, Scotland, U.K. (xiao.xu@ed.ac.uk, sasa.djokic@ed.ac.uk).

A. J. Collin, R. Langella and A. Testa are with the University of Campania "Luigi Vanvitelli", Aversa, Italy (adam.collin@ieee.org, roberto.langella@unicampania.it, alfredo.testa@unicampania.it)

II. REPRESENTATION OF PC-SMPS OPERATING CYCLE

An important aspect of analyzing the performance of PC-SMPS' is that manufacturers' specifications are usually given for PC-SMPS' operating at rated power, while in practice their operating powers vary in a wide range, depending on specific performed tasks (mostly from 20%-60% of P_{rated} [19, 20]). This is denoted as a "PC operating cycle" and is illustrated in Fig. 1, using an example of a PC in a commercial office setting [20].

In order to correctly evaluate the overall operational and power quality performance of a PC-SMPS, its operating cycle must be considered. The bar plot in Fig. 1 shows four discrete operating power levels of 100%, 50%, 20% and 10% of P_{rated}, which represent four general types of activities, together with corresponding durations of activities for a PC in a commercial office. Ranges around the discrete values are also indicated in Fig. 1 as: a) 2%-10%, very low power mode (stand-by or idling), b) 10%-30%, low power mode (non-demanding text processing, internet browsing), c) 30%-70%, medium power mode (typical office tasks, read/write operations), and d) 70%-100%, high power mode (streaming, complex simulations).

Generally, the operating cycle may be specified in either PMF or PDF form. To illustrate that the presented approach can use both forms, the conversion of the PMF in Fig. 1 into a PDF is obtained by discretizing four power ranges into a series of individual power levels with a 1% P_{rated} interval. The discrete powers within each power range are assumed to follow a normal distribution, with a coverage probability of 99.7% and sum of their values equal to corresponding percentages of total duration. The weighting coefficients for discrete powers are represented by the mix of normal distributions in Fig. 2 (more details in Table VI in Appendix). The conversion from PMF to PDF is trivial, as it requires a simple discretization. Although the operating cycles for different PC users will vary, the specification of different operating cycles (theoretical or measured) does not affect generality of presented methodology.

III. METHODOLOGY FOR EVALUATING OPERATING CYCLE PERFORMANCE AND POWER QUALITY INDICES

The PC-SMPS operational characteristics and power quality indices analysed in this paper are: total efficiency η, fundamental efficiency η_1, true, displacement and distortion power factors PF, PF_1 and PF_d, total subgroup current harmonic distortion ($THDS_I$) and total subgroup harmonic current $THCS$, for harmonic subgroup orders 2-40, total subgroup current interharmonic distortion $TIHDS_I$ and total subgroup interharmonic current $TIHCS$, for interharmonic subgroup orders 0-40. The reference measurement method for harmonic and interharmonic measurements and its parameters (window length, target uncertainty, etc.) are taken from [3] and [21]; the metrics for distorted powers are taken from [22].

A sequence of discrete intervals τ forms the operating cycle T. Operating power level $P^{(j)}$ at power demand j of a PC-SMPS will have a cumulative duration $\tau^{(j)} = \sum_i \tau_i$, with $\tau_i: P = P^{(j)}$, so total duration of the operating cycle is: $T = \sum_{j=1}^{N_P} \tau^{(j)}$, where N_P is total number of different operating powers, $P^{(j)}$. The generic frequency of occurrence of N_P different power levels $P^{(j)}$ is $f^{(j)} = \tau^{(j)}/ T$, and each $P^{(j)}$ will have cumulative duration $\tau^{(j)}$ and frequency of occurrence $f^{(j)}$.
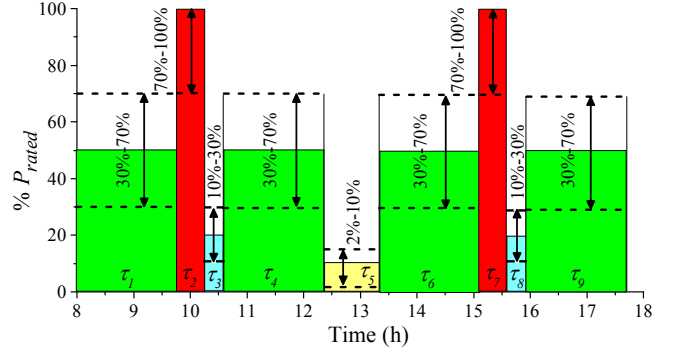

Fig. 1. Example of a PC operating cycle in a commercial office setting; bar plot represents discrete values [20], dash lines indicate ranges [12].
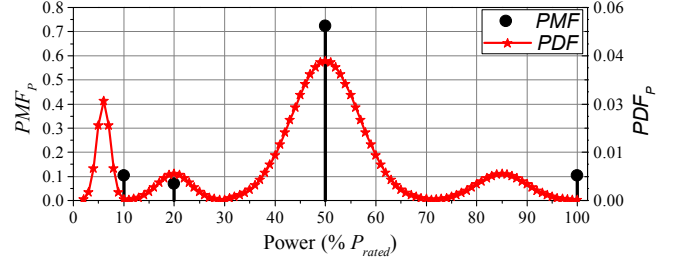

Fig. 2. Probability mass and density functions for Fig. 1.

A. Single Operating Power Scenario

The total and fundamental efficiencies of a PC-SMPS operating at a constant power $P^{(j)}$ of the operating cycle are:

$$\eta_P^{(j)} = P_{dc}^{(j)}/P_{ac}^{(j)}, \tag{1}$$

$$\eta_{P1}^{(j)} = P_{dc}^{(j)}/P_{ac,1}^{(j)}, \tag{2}$$

where the active powers are:

$$P_{dc}^{(j)} = \frac{1}{N^{(j)}} \sum_{m=1}^{M} \sum_{n=1}^{N^{(j)}} v_{dc,m}(n) i_{dc,m}(n), \tag{3}$$

$$P_{ac}^{(j)} = \frac{1}{N^{(j)}} \sum_{n=1}^{N^{(j)}} v_{ac}(n) i_{ac}(n), \tag{4}$$

$$P_{ac,1}^{(j)} = \frac{1}{N^{(j)}} \sum_{n=1}^{N^{(j)}} v_{ac,1}(n) i_{ac,1}(n), \tag{5}$$

and v_{ac} and i_{ac} are the sampled ac voltage and current, with fundamental components $v_{ac,1}$ and $i_{ac,1}$, while $v_{dc,m}$, $i_{dc,m}$ are the dc voltage and dc current at dc output level m of total M dc output levels, over the observation period $\tau^{(j)}$ constituted by $N^{(j)}$ samples equal to $\tau^{(j)} f_s$, where f_s is the sampling frequency.

For the calculation of operating power factors and power quality indices, the following equations are used:

$$PF^{(j)} = P_{ac}^{(j)}/S_{ac}^{(j)}, \tag{6}$$

$$PF_1^{(j)} = P_{ac,1}^{(j)}/S_{ac,1}^{(j)}, \tag{7}$$

$$PF_d^{(j)} = PF^{(j)}/PF_1^{(j)}, \tag{8}$$

where: $S_{ac}^{(j)} = V_{ac}^{(j)} I_{ac}^{(j)}$, $V_{ac}^{(j)}$ and $I_{ac}^{(j)}$ are the rms values of the corresponding input ac voltage and ac current and $S_{ac,1}^{(j)} = V_{ac,1}^{(j)} I_{ac,1}^{(j)}$, represent the fundamental components. Furthermore:

$$THDS_I^{(j)} = \frac{\sqrt{\sum_{h=2}^{40} I_{sg,h}^2}}{I_{sg,1}}, \tag{9}$$

$$THCS^{(j)} = \sqrt{\sum_{h=2}^{40} I_{sg,h}^2}, \tag{10}$$

$$TIHDS_I^{(j)} = \frac{\sqrt{\sum_{h=0}^{40} I_{isg,h}^2}}{I_{sg,1}}, \tag{11}$$

$$TIHCS^{(j)} = \sqrt{\sum_{h=0}^{40} I_{isg,h}^2}, \tag{12}$$

where: $I_{sg,h}$, $I_{isg,h}$ - harmonic and interharmonic subgroups [3].

B. Entire Operating Cycle Scenario

For given operating cycle of a PC, each quantity defined by (1)-(12) can be associated with the cumulative duration $\tau^{(j)}$ and frequency of occurrence $f^{(j)}$ of the corresponding power $P^{(j)}$. For efficiency calculation, it is useful to use "energy efficiency":

$$\eta_E = \frac{\sum_{j=1}^{N_P} \left(P_{dc}^{(j)}\right) \cdot \tau^{(j)}}{\sum_{j=1}^{N_P} P_{ac}^{(j)} \tau^{(j)}} = \frac{E_{dc}}{E_{ac}}, \tag{13}$$

$$\eta_{E1} = \frac{\sum_{j=1}^{N_P} \left(P_{dc}^{(j)}\right) \cdot \tau^{(j)}}{\sum_{j=1}^{N_P} P_{ac,1}^{(j)} \tau^{(j)}} = \frac{E_{dc}}{E_{ac,1}}, \tag{14}$$

where: $E_{(.)}$ is energy consumed at power $P_{(.)}$ by a customer using PC for performing range of specific activities and tasks.

For calculating the operating power factors, mean quantities can be used. (Note: Energy billing in some countries, e.g. Italy, uses (14), while standard [22] suggests (15)-(16)):

$$\overline{PF} = \frac{\sum_{j=1}^{N_P} P_{ac}^{(j)} \tau^{(j)}}{\sum_{j=1}^{N_P} S_{ac}^{(j)} \tau^{(j)}}, \tag{15}$$

$$\overline{PF}_1 = \frac{\sum_{j=1}^{N_P} P_{ac}^{(j)} \tau^{(j)}}{\sum_{j=1}^{N_P} S_{ac,1}^{(j)} \tau^{(j)}}, \tag{16}$$

$$\overline{PF}_d = \frac{\overline{PF}}{\overline{PF}_1}. \tag{17}$$

For the representation of harmonics, two parameters are required for each operating state, j: a) harmonic magnitude, $I_h^{(j)}$, and b) harmonic phase angle, $\phi^{(j)}$. Significant variations of harmonic and interharmonic currents of PC-SMPS operating at different powers $P^{(J)}$ will require to process and store the results in the form of two matroids: $[P^{(J)}, h, I_{sg,h}]$ and $[P^{(J)}, h, I_{isg,h}]$, each of dimension N_P x N_h x N_{Ih}, where N_{Ih} is the number of discrete consecutive classes in which measured values of currents are discretized.

Using the above approach, 2x41 PMFs are obtained, each referring to a specific (inter)harmonic subgroup, including dc and fundamental components. From this, relevant statistical characteristics for each PMF can be extracted: maximum, mean, mode and 95th percentile values, which are, respectively:

$$\hat{I}_{sg,h} = \max_j I_{sg,h}^{(j)}, \tag{18}$$

$$\mu_{I_{sg,h}} = \sum_{j=1}^{N_P} I_{sg,h}^{(j)} \cdot f^{(j)}, \tag{19}$$

$$\upsilon_{I_{sg,h}} = I_{sg,h}^{(j^*)} : j^* \to max_j f^{(j)}. \tag{20}$$

$$I_{sg,h,95\%} = I_{sg,h}^{(j^*)} : j^* \to \sum_j f^{(j)} \geq 95\%. \tag{21}$$

These equations can be used to evaluate the overall operational and PQ performance of a PE device over its entire operating cycle, (see (22) and (23) in Section VI.B).

IV. TESTING AND MEASUREMENT FRAMEWORK

A. Test Set-Up

Fig. 3 shows the fully automated test-bed used for testing, consisting of: a control PC, a voltage source, two oscilloscopes for data acquisition, four current probes, four voltage probes and two variable resistors for adjusting PC-SMPS' operating power from 1-100% of P_{rated}, at ±12 V and ±5 V dc outputs. Although the dc power output in practical applications may fluctuate continuously, the dc power was controlled with negligible variation. All recordings are synchronized by the data acquisition system with a sampling rate of 1 MSa/s.

B. Supply Voltage Waveforms Applied in Tests

Fig. 4 shows the three supply voltage waveforms used in tests, denoted as WF1, WF2 and WF3. WF1 was a reference, ideally sinusoidal voltage supply, while two distorted voltage waveforms, WF2 and WF3, were derived from measurements in low-voltage networks. Further details are available in [15].

C. Evaluation of Measurement Accuracy and Uncertainties

To evaluate the measurement accuracy and uncertainty, the calculation approach from [13] was applied. This process starts from the manufacturer standard uncertainties given in Table I. Based on these values uniformly distributed random errors were obtained for each instrument and used to perform Monte Carlo (MC) trials to assess the error distribution characteristics of the calculated indices. The forcing terms, i.e. the voltage waveform and dc load, were calibrated to ensure a negligible error and were not considered in the uncertainty evaluation.
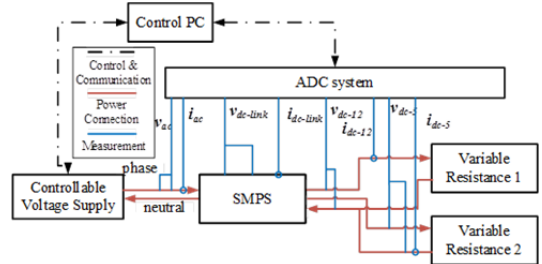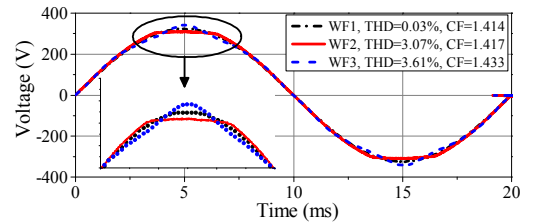

Fig. 3. A fully automated PC-SMPS test set-up.

Fig. 4. The three voltage waveforms used in tests (CF denotes crest factor).

TABLE I. STANDARD UNCERTAINTIES (MANUFACTURERS' DATASHEETS).

Measurement	Equipment	$E_{reading}$	E_{range}	Ref.
v_{ac}	Differential probe	±2%	/	[23]
i_{ac}	Current probe	±0.5%	/	[24]
$v_{dc\text{-}12}$	Differential probe	±2%	/	[23]
$i_{dc\text{-}12}$	Current probe	±1%	±2mA	[25]
$v_{dc\text{-}5}$	Differential probe	±2%	/	[23]
$i_{dc\text{-}5}$	Current probe	±1%	±2mA	[25]
Data acquisition	ADC system	±0.03%	dc: ±0.02%±2mV ac: ±0.02%	[26]
$E_{reading}$, E_{range}: reading and range uncertainty; ADC system range: ±100 V.				

To evaluate the impact of measurement uncertainty on the error distribution characteristics of the calculated indices, the reference voltage and current waveforms are used, with the rms values for v_{ac} and i_{ac} of 230 V and 2.182 A, corresponding to a reference power of $P_{ac,ref}$=500 W. The reference dc voltage and current values for v_{dc-12}, v_{dc-5}, i_{dc-12}, i_{dc-5} are 12 V, 5 V, 25 A, and 20 A, respectively, corresponding to the total reference dc power of $P_{dc,ref}$ = 400 W. A reference efficiency of 80% was selected, i.e. the actual efficiency of PC-SMPS1 operating at P_{rated}. The error distribution characteristics were evaluated at 100%, 70%, 50%, 30%, 10% and 2% of P_{rated}, where reference values for the ac and dc side voltage and current waveforms were scaled-down from the corresponding values at 100% of P_{rated}. The reference ac voltage and current waveforms were purely sinusoidal, with current lagging five degrees (5°) with respect to the voltage. After performing 50,000 MC trials, histograms of the ac power deviation ($\Delta P_{ac}/P_{ac,ref}$), dc power deviation ($\Delta P_{dc}/P_{dc,ref}$), efficiency and fundamental efficiency deviation ($\Delta\eta/\eta_{ref}$ and $\Delta\eta_1/\eta_{1,ref}$ respectively) were obtained. Results at 100% of P_{rated} are shown in Fig. 5.

Table II lists the expanded uncertainty values (coverage factor 3) used to evaluate the measurement precision. In terms of the accuracy constraints and errors introduced by the available measurement equipment, the cumulative effects of these uncertainties are comparable with the requirements from [12], and are, therefore, considered acceptable, particularly as the probabilities of operation at lower powers in the considered PC-SMPS operating cycle are low, so a larger uncertainty observed for PC-SMPS' operating at these powers will not affect the presented results.

V. MEASUREMENT RESULTS

The analysis and results presented in this paper are obtained using two desktop PC power supply units: PC-SMPS1, with P_{rated} = 400 W, and PC-SMPS2 with P_{rated} = 350 W.

A. Lost Periodicity in PC-SMPS Applications

Standards [3, 21] stipulate the use of a time-window of exactly 10 fundamental periods in 50 Hz supply systems and 12 periods in 60 Hz supply systems. Figs. 6 and 7 compare the current (inter)harmonic spectra for 200 ms window length with the results for 3 s (suggested in [21]) and 8.4 s (this paper) windows. For the latter two, squared average values from 15 and 42 consecutive individual 200 ms windows are used [3]. The 8.4 s window corresponds to 420 fundamental periods in 50 Hz supply systems (504 periods in 60 Hz supply systems) and main reason for its selection is that it allows for integer factorization of 420 and 504 periods by most of the pairs from the series {1, 2, 3, 4, 5, 6, 7}, which would produce correct results for all combinations of current and voltage periods from that series.

TABLE II. EXPANDED UNCERTAINTY (COVERAGE FACTOR 3) AT DIFFERENT POWER LEVELS.

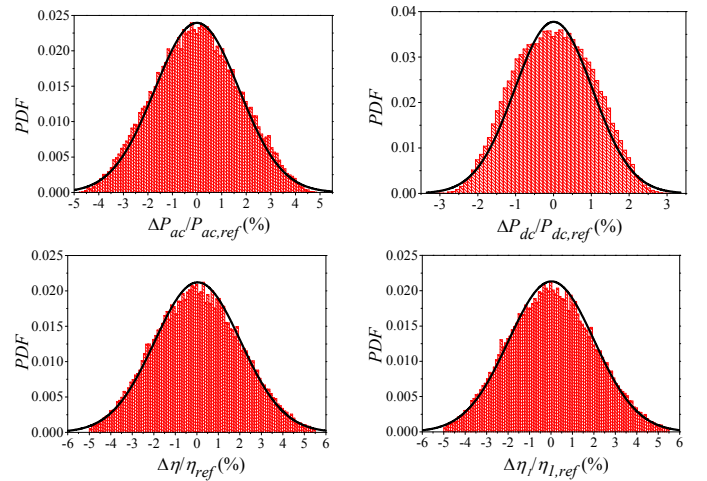| % P_{rated}	Expanded Uncertainty in %			
	$\Delta P_{ac}/P_{ac,ref}$ (%)	$\Delta P_{dc}/P_{dc,ref}$ (%)	$\Delta\eta/\eta_{ref}$ (%)	$\Delta\eta_1/\eta_{1,ref}$ (%)
70-100	[5.41, 5.15]	[3.11, 3.09]	[6.25, 5.99]	[6.25, 6.00]
50-70	[5.86, 5.41]	[3.10, 3.11]	[6.62, 6.25]	[6.62, 6.25]
30-50	[7.23, 5.86]	[3.15, 3.10]	[7.90, 6.62]	[7.91, 6.62]
10-30	[16.66, 7.23]	[3.40, 3.15]	[17.13, 7.90]	[17.13, 7.91]
2-10	[79.90, 16.66]	[7.07, 3.40]	[95.14, 17.13]	[95.16, 17.13]

Fig. 5. Histogram and fitted normal distributions for: ac power deviation, dc power deviation, efficiency and fundamental efficiency deviation, for PC-SMPS1 with $P_{dc,ref}$= 400 W.

B. Discussion of Lost Periodicity Results

For PC-SMPS1 operating above 50% of P_{rated}, input ac current, i_{ac}, has the same 20 ms period as the input ac voltage, v_{ac}, while the output dc voltage, v_{dc}, features a characteristic 100 Hz voltage ripple with a 10 ms period. However, when the operating power of PC-SMPS1 reduces below around 50% of P_{rated}, the phenomena of lost periodicity is observed, with the period of i_{ac} increasing from 20 ms to 60 ms (period-tripling, or period-3). This is shown in Figs. 6a and 6b overleaf, where the dc link capacitor takes longer time to discharge, resulting in a dc voltage ripple period of 30 ms. Under these conditions, the use of 200 ms window length will produce an error in 50 Hz supply systems, as there will be three possible different current waveform samples within 10 consecutive periods of 200 ms window. However, this will not happen in 60 Hz supply systems, where the ac voltage supply has a period of 50/3 ms and period-tripling of current results in the period of 50 ms, i.e. in exactly 12 voltage and 4 current periods in 200 ms window.

Fig. 6c illustrates an example with periodicity of input ac current changing to 140 ms, i.e. period septupling, or period-7, when the dc voltage ripple features a much longer 70 ms period. This example justifies the use of the 8.4 s window, as the 50/7 component (marked with a circle in Fig. 6c) will not be correctly captured with the two other windows. If PC-SMPS1 power reduces below around 10% of P_{rated}, the period of i_{ac} will change to 40 ms (Fig. 6d, period doubling, or period-2, when dc link capacitor voltage ripple period is 40 ms).

If PC-SMPS1 operating power further decreases (below 3% of P_{rated}), there is a completely lost periodicity of input ac current ("chaotic operation" [15]). In terms of the dc component, Fig. 6d indicates the presence of a very high non-zero mean value of around 150 mA, which is of concern, as it can lead to serious problems (transformer saturation, or malfunction of protection). The results for PC-SMPS2 in Fig. 7 are similar: the input ac current has 20 ms period until the operating power drops below around 7%, Fig. 7a, when it becomes heavily distorted. Fig. 7b confirms the occurrence of period-septupling, while Fig. 7c illustrates a quasi-aperiodic operation of PC-SMPS2.
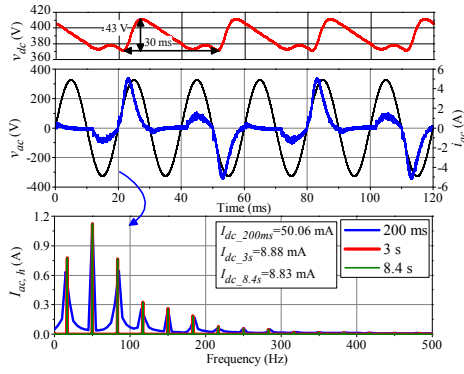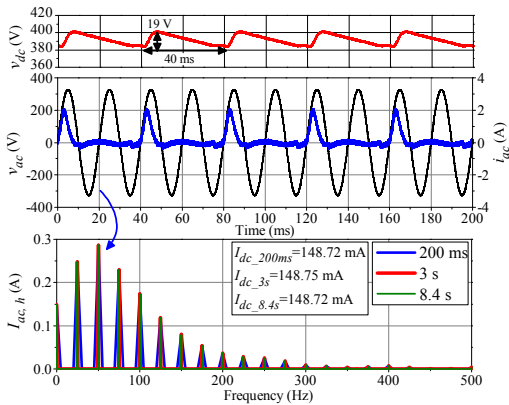
a) 50% P_{rated} (lost periodicity: triple-period, or period-3 current)
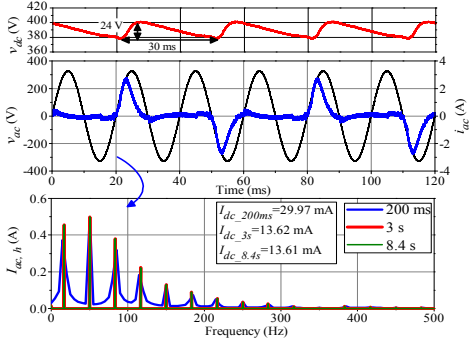
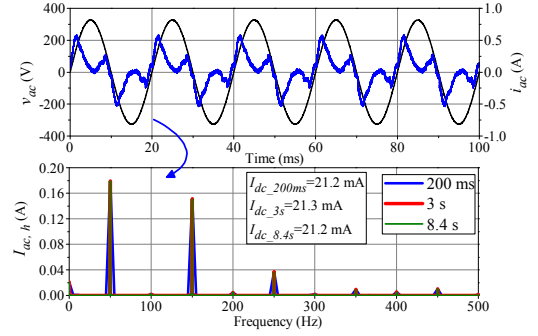b) 20% P_{rated} (lost periodicity: triple-period, or period-3 current)
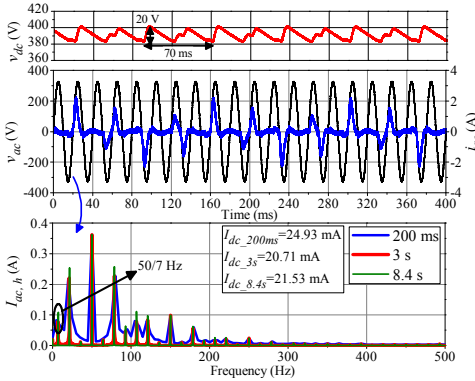
c) 14% P_{rated} (lost periodicity: septuple-period, or period-7 current)
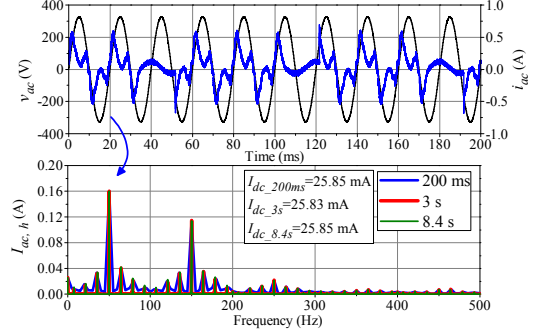

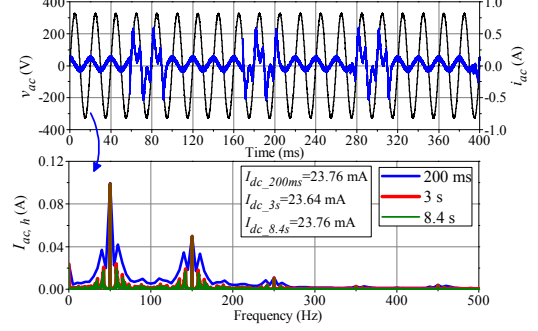d) 10% P_{rated} (lost periodicity: double-period, or period-2 current)

Fig. 6.   The illustration of the lost periodicity phenomena, PC-SMPS-1.

a) 7% P_{rated} (preserved periodicity)

b) 6% P_{rated} (lost periodicity: septuple-period, or period-7 current)

c) 2% P_{rated} (lost periodicity: quasi-aperiodic current)

Fig. 7.   The illustration of the lost periodicity phenomena, PC-SMPS-2.

Figs. 6 and 7 both demonstrate that lost periodicity may result in a particularly strong emission of subharmonics, interharmonics and the dc component, which are not captured with a 200 ms window. Period-tripling (Figs. 6a and 6b) results in a significant increase of 50/3 Hz subharmonic and its odd multiple interharmonics (250/3 Hz, 350/3 Hz,...), while the 50/2 Hz subharmonic and its odd multiple interharmonics (150/2 Hz, 250/3 Hz,…) occur for period-doubling (Fig. 6d). For period-septupling (Figs. 6c and 7b), a 50/7 subharmonic occurs, together with its odd multiple sub/inter harmonics.

C. Evaluation of PC-SMPS Performance for Sinusoidal and Distorted Voltage Supply

Fig. 8 further investigates the impact of lost periodicity, on the dc component and subgroup current (inter)harmonics (up to the order of 10) for a number of operating powers and for three different supply voltage waveforms WF1-WF3. Window length of 8.4 s is used to avoid potential problems with spectral leakage. It can be seen from Fig. 8 that the dc component, subharmonics and 2nd harmonic significantly increase when the operating power reduces to around 50% of P_{rated}, when they become the dominant components in the spectrum.

For the operating power range 50%-100% of P_{rated}, the 3rd and 5th harmonics are dominant components, which gradually decrease with the decreasing operating power. There is a distinctive step change in waveform distortion at around 50% of P_{rated}, when lost periodicity starts to occur. It can be seen that the presence of the supply voltage distortion (results for WF2 in Fig. 8b and WF3 in Fig. 8c) has only a small impact on the dc component and current (sub/inter)harmonic emission of PC-SMPS1 (similar results are obtained for PC-SMPS2.

D. Evaluation of PC-SMPS Operating Cycle Performance

In order to check if the recommended 200 ms window from [3] can be used for the correct calculation and evaluation of PC-SMPS' performance, Fig. 9 shows efficiencies, true power factor and selected PQ indices at different operating powers calculated with different window lengths, again for WF1-WF3. Combined standard uncertainty bounds are represented by the error bars in Figs. 9a and 9b, but are not shown in Figs. 9c-9f as they are very small (less than 1%).

Fig. 9 clearly indicates a steep change in PF, $TIHDS_I$ and I_{DC} values at around 50 % of P_{rated}, as well as a fast reduction in η and η_1 efficiencies and increase in $THDS_I$ values below 20 % of P_{rated}. This confirms that the assessment of PC-SMPS1 operational and PQ performance based on a few fixed discrete operating powers may not accurately represent the actual device performance during the entire operating cycle. Table III shows the ± Min/Max percentage differences between individual 200 ms and 3 s windows from the results for 8.4 s 8 window. When lost periodicity occurs, the differences increase (especially for $THDS_I$ and $THCS$) and are influenced by WF2-WF3 voltage. For $TIHDS_I$, $TIHCS$ and I_{DC}, the observed differences are significant, demonstrating the importance of selecting a suitable window length.

TABLE III. DIFFERENCE (IN %) OF 200 MS AND 3 S FROM 8.4 S WINDOW

Window	η	η_1	PF	PF_1	PF_d	$THDS_I$	$THCS$	$TIHDS_I$	$TIHCS$	I_{DC}
200ms	-20	-21	-17	-10	-10	-45	-47	-27	-27	-1E^2
	25	22	17	11	15	46	57	32	31	2E^3
3s	-1.0	-1.3	-2.5	-0.9	-1.9	-4.6	-5.3	-3.8	-3.7	-9.2
	2.0	1.8	2.7	0.6	2.2	4.8	5.5	4.0	3.9	1E^3

a) WF1

b) WF2

c) WF3

Fig. 8. The dc component, current harmonic, subharrmonic and interharmonic magnitudes for PC-SMPS-1 (8.4 s window).

a) η

b) η_1

c) PF

d) $THDS_I$

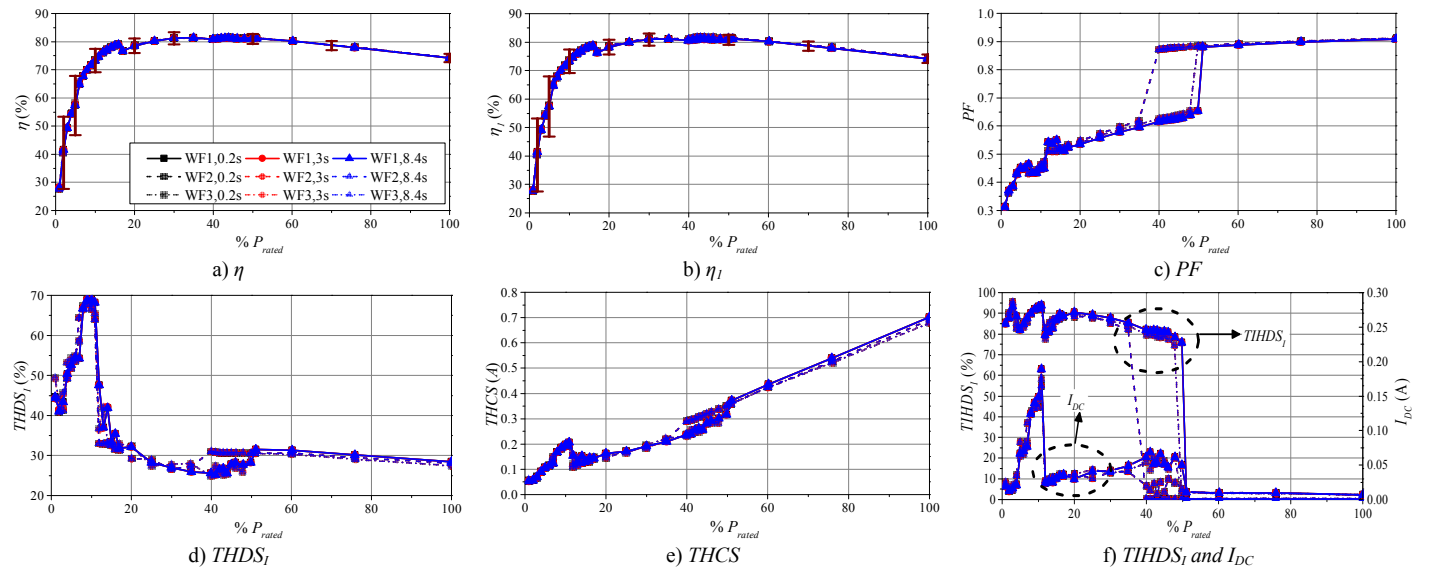e) $THCS$

f) $TIHDS_I$ and I_{DC}

Fig. 9. Performance indicators and power quality indices with standard uncertainty bounds obtained from 200 ms, 3 s and 8.4 s time windows (PC-SMPS1).
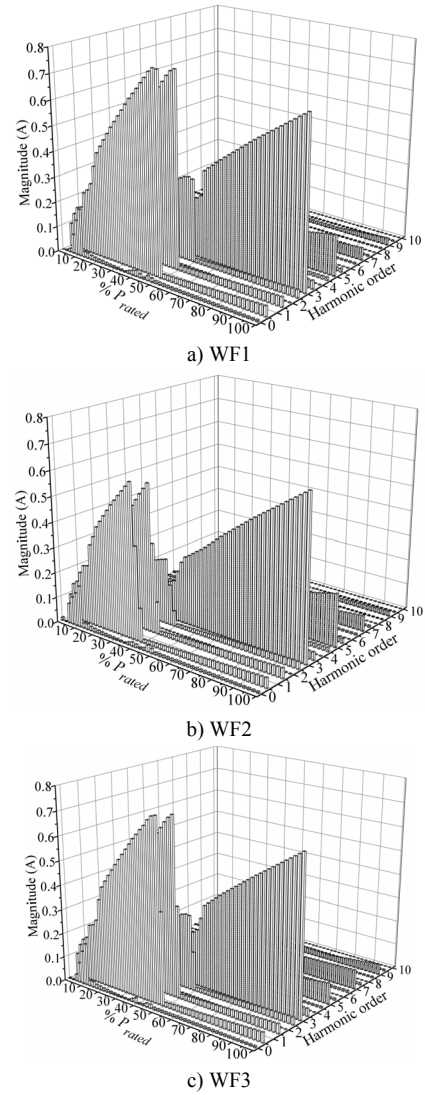
VI. RESULTS FOR PC-SMPS OPERATING CYCLE PERFORMANCE

Although the results for PC-SMPS1 performance in Fig. 9 provide detailed information on the changes in PC-SMPS characteristics, they cannot indicate the overall operating cycle performance. For this purpose, the information on PE device performance at specific operating power levels can be combined with the corresponding frequency of occurrence data. In this paper, the PMF and PDF data in Fig. 2 are used to demonstrate the methodology presented in Section III.

A. Operating Cycle Performance: Discrete Operating Powers and Normally Distributed Ranges of Operating Powers

The PMFs and PDFs for PC-SMPS1 operating cycle based characteristics under WF1-WF3 are shown in Figs. 10 and 11. For the operating cycle performance under discrete operating powers in Fig. 10, PC-SMPS1 has the highest η and η_1 at medium power (50% of P_{rated}) and lower η and η_1 at 10% and 100% of P_{rated}. $THDS_I$ values at 20%, 50% and 100% of P_{rated} are very close, while the highest $THDS_I$ value is at 10% P_{rated}. $THCS$ values generally decrease with decreasing power, except at very low power, where $THCS$ slightly increases. $TIHDS_I$ and $TIHCS$ values are negligible until lost periodicity occurs, when they increase significantly. All indices have the greatest height, i.e. the highest probability, at 50% of P_{rated}. The supply voltage distortion has little impact on the PC-SMPS performance.

For normally distributed operating powers in Fig. 11, η and η_1 generally increase with increasing power, while $THCS$ almost linearly decreases with reducing power. $THDS_I$ is almost constant at higher powers, with an apparent increase at very low operating powers. When lost periodicity occurs, $TIHDS_I$ and $TIHCS$ exhibit a step change. As with Fig. 10, the indices at around 50% P_{rated} have the highest probability.

B. Operating Cycle Performance: Weighted Indices

Based on the percentage of time spent at each operating power with respect to the total duration of the operating cycle and values calculated using 8.4 s window at different operating powers in Fig. 9, the overall PQ indices are calculated and listed in Table IV. The calculation procedure is illustrated for the mean weighted true power factor (PF_μ) in (22) and (23) for discrete operating powers and operating cycle with the ranges of normally distributed powers, respectively.

$$PF_\mu = k_{P10}PF_{P10} + k_{P20}PF_{P20} + k_{P50}PF_{P50} + k_{P100}PF_{P100} \quad (22)$$

$$PF_\mu = \sum_{k=1}^{100} k_{Pk}PF_{Pk} \quad (23)$$

where: k_{P10}, k_{P20}, k_{P50} and k_{P100} are the weighting coefficients from Table VI, and PF_{P10}, PF_{P20}, PF_{P50}, and PF_{P100} are the measured PF at the four corresponding operating powers. k_{Pk} and PF_{Pk} are the weighting coefficients and measured PF.
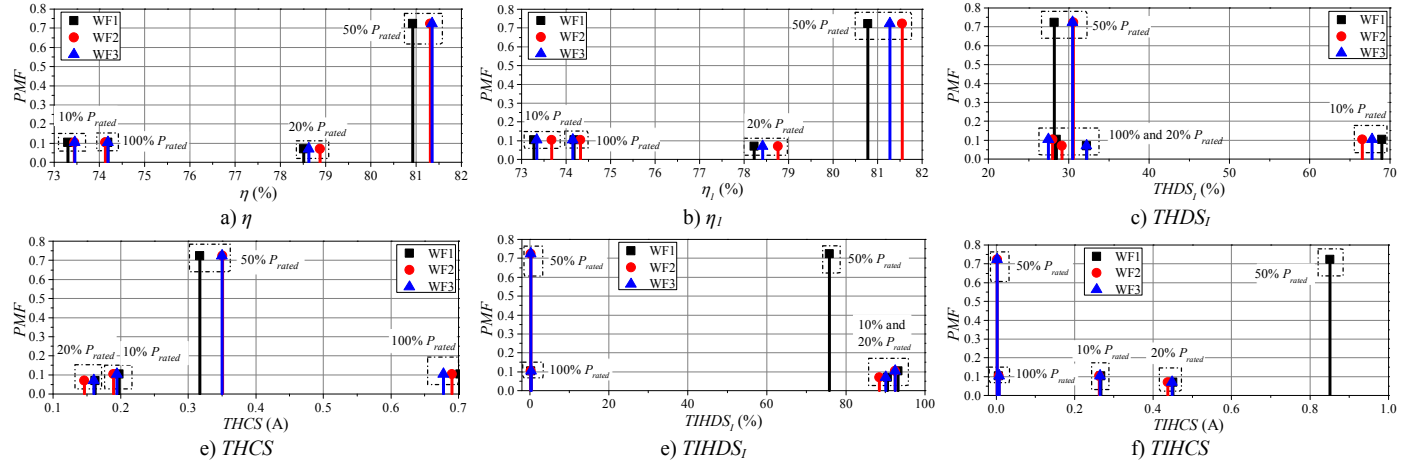

Fig. 10. Operating cycle performance of PC-SMPS1 for WF1-WF3 and for operating cycle represented with discrete powers (PMF) in Fig. 2.
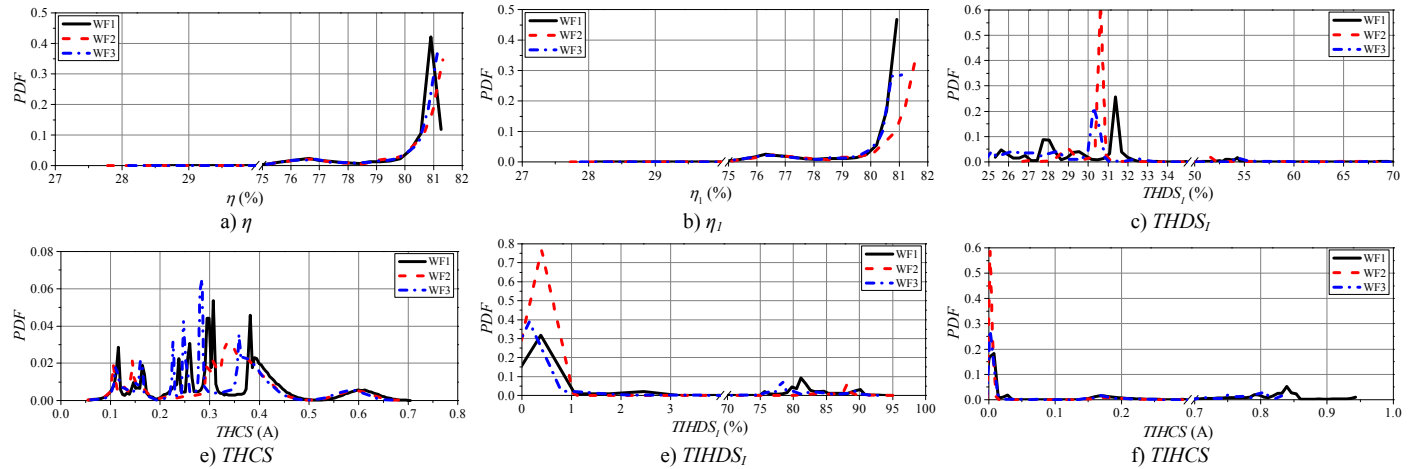

Fig. 11. Operating cycle performance of PC-SMPS1 for WF1-WF3 and for operating cycle represented with ranges of normally distributed powers (PDF) in Fig. 2.

In (22), k_{Pk} corresponds to the frequency of occurrence values in Table VI, while in (23) k_{Pk} values are the frequency of occurrence values that can be deducted from the PDF in Fig. 2. It is worth noting that (22) and (23) are equivalent to (19).

The values in Table IV summarize the expected performance over the entire operating cycle of PC-SMPS1 for all considered indices, while the values obtained at P_{rated} are displayed in Table V. By comparing the weighted PQ indices (Table IV) with the PQ indices at rated power (Table V), it can be seen how it would be possible to overestimate (or underestimate) the PQ performance when considering only P_{rated}. It is clear from Tables IV and V that there are differences between the most of the calculated values, with noticeable differences between the rated and weighted operating cycle values of total and fundamental efficiencies and true/distortion power factors. As expected, pronounced differences are observed between the rated and weighted operating cycle values of dc current and interharmonic/subharmonic emission.

Finally, Fig. 12 provides a comparison of operating cycle based values of PC-SMPS1 current harmonic spectra with the corresponding values when it is operating at rated power and with the max/min values observed from all test points (i.e. all operating powers and voltage waveforms). Again, the differences discussed above are clearly visible. Existing limits from [9] are also indicated. These results suggest that harmonic emission during actual operation can be higher than at P_{rated}, clearly indicating that the changes in the characteristics for the range of actual or expected operating powers (defined in this paper as the "operating cycle performance") could be considered as a part of standard device assessment procedures.

TABLE IV. OPERATING CYCLE BASED POWER QUALITY AND PERFORMANCE INDICATORS OF PC-SMPS1.

	$I_{dc,\mu}$ (mA)	η_μ (%)	$\eta_{1,\mu}$ (%)	PF_w	$PF_{1,\mu}$	$PF_{d,\mu}$	$THDS_{I,\mu}$ (%)	$THCS_\mu$ (A)	$TSHDS_{I,\mu}$ (%)	$TSHCS_\mu$ (mA)	$TIHDS_{I,\mu}$ (%)	$TIHCS_\mu$ (mA)
	Discrete Operating Powers											
WF1	54	79	79	0.65	0.94	0.69	33	0.33	64	607	71	680
WF2	28	80	80	0.82	0.92	0.89	33	0.36	15	55	16	60
WF3	26	80	80	0.82	0.92	0.89	34	0.36	15	57	16	61
	Ranges of Normally Distributed Operating Powers											
WF1	35	78	78	0.72	0.92	0.78	32	0.33	42	333	46	360
WF2	24	78	79	0.81	0.91	0.88	33	0.34	16	61	17	67
WF3	32	78	78	0.74	0.92	0.80	32	0.32	37	276	40	297

TABLE V. POWER QUALITY AND PERFORMANCE INDICATORS OF PC-SMPS1 AT RATED POWER.

WF	I_{dc} (mA)	η (%)	$\eta_{1,}$ (%)	PF	PF_I	PF_d	$THDS_I$ (%)	$THCS$ (A)	$TSHDS_I$ (%)	$TSHCS$ (mA)	$TIHDS_I$ (%)	$TIHCS$ (mA)
1	7.1	74	74	0.91	0.95	0.96	29	0.70	0.06	1.6	0.26	6.3
2	6.6	74	74	0.91	0.95	0.96	28	0.69	0.07	1.6	0.29	7.1
3	6.7	74	74	0.91	0.95	0.96	27	0.68	0.08	1.9	0.29	7.1
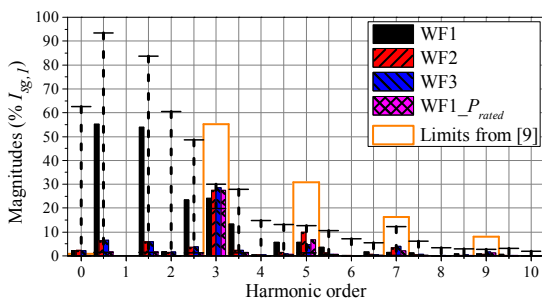
a) discrete operating powers
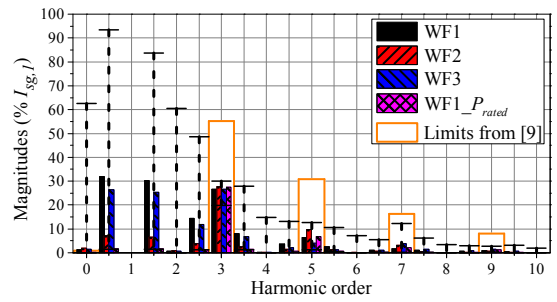
b) ranges of normally distributed operating powers

Fig. 12. The weighted current harmonic spectra of PC-SMPS1 for WF1-3, where the whisker plot shows the range of values measured during the tests.

VII. CONCLUSIONS

This paper has presented a novel methodology to evaluate the overall operational and power quality performance of a PC-SMPS by considering their entire operating cycles. The measurement procedure was discussed and evaluated in terms of the test set-up requirements and uncertainties due to accuracy constraints and errors introduced by the available measurement equipment. The presented results have shown that the correct assessment of PC-SMPS performance cannot rely on a single (or a few) observation points, and that particular care should be taken during the operation at low powers, when PC-SMPS' input ac current may lose its periodicity with the supply voltage frequency. In such cases, there is a significant increase of PC-SMPS' current waveform distortion, at harmonic and interharmonic frequencies, and a substantial decrease of efficiency and power factors.

The presented testing and evaluation methodology has been demonstrated on the example of PC-SMPS', but can be easily applied for the analysis of other types of PE devices that operate with variable powers. For example, a similar case of lost periodicity phenomena has been reported for PV inverter in [3] and the authors are currently considering applying the presented methodology for a more comprehensive assessment of the entire operating cycle performance of PV inverters. In this context, the presented analysis and results provides a new perspective for assessing performance of PE devices and contributes to the ongoing efforts at international level aimed at developing comprehensive and standardized testing procedures for operational and power quality performance evaluation.

VIII. APPENDIX

TABLE VI. EXAMPLE DATA FOR PC OPERATING CYCLE USED FOR ANALYSIS.

PC Operating State	% of P_{rated}	Duration (hours)	% of Total Duration		
Four Discrete Powers					
Full load	100	1	10.34%		
Typical load	50	7	72.41%		
Light load	20	0.67	6.91%		
Low load	10	1	10.34%		
Ranges of Operating Powers				*Normal Distribution*	
				μ	3σ
High Power Range	70-100	1	10.34%	85	15
Medium Power Range	30-70	7	72.41%	50	20
Low Power Range	10-30	0.67	6.91%	20	10
Very Low Power Range	2-10	1	10.34%	6	4

REFERENCES

[1] Office for National Statistics (UK), "Percentage of households with home computers in the United Kingdom (UK) from 1985 to 2014."

[2] Office for National Statistics (UK), "Frequency with which individuals used the computer in Great Britain from 2006 to 2015."

[3] *EMC: Testing and measurement techniques-General guide on harmonics and interharmonics measurements and instrumentation, for power supply systems and equipment connected thereto*, IEC Std. 61000-4-7, 2009.

[4] X. Xu, A. J. Collin, S. Z. Djokic, S. Yanchenko, F. Möller, J. Meyer, R. Langella, A. Testa, "Analysis and modelling of power-dependent harmonic characteristics of modern PE devices in LV networks", *IEEE Trans. Pow. Delivery*, vol. 32, no. 2, pp.1014-1023, Apr. 2017.

[5] X. Xiao, S. Djokic, R. Langella and A. Testa, "Performance comparison of three main SMPS types under sinusoidal and distorted supply voltage," *2017 IEEE PowerTech Conf.*, Manchester, UK, Jun. 2017.

[6] ENERGY STAR Certification Criteria [Online], Available: https://www.energystar.gov/products/office_equipment/computers/key_product_criteria

[7] 80 PLUS Certification Criteria [Online], Available: https://www.plugloadsolutions.com/docs/collatrl/print/Generalized_Internal_Power_Supply_Efficiency_Test_Protocol_R6.7.pdf

[8] COMMISSION REGULATION (EU) No 617/2013, Implementing Directive 2009/125/EC of the European Parliament and of the Council with regard to ecodesign requirements for computers and computer servers. Jul. 2013. [Online]. Available: http://data.europa.eu/eli/reg/2013/617/oj

[9] *Electromagnetic Compatibility (EMC) – Part 3-2: Limits for harmonic current emissions (equipment input current ≤16 A per phase)*, IEC Std 61000-3-2, 2014.

[10] R. Hotopp, Private Photovoltaik-Stromerzeugungsanlagen im Netzparallelbetrieb: Planung, Errichtung, Betrieb, Wirtschaftlichkeit, Essen, Germany: RWE, 1991.

[11] W. Bower, C. Whitaker, W. Erdman, M. Behnke, and M. Fitzgerald, "Performance test protocol for evaluating inverters used in grid-connected photovoltaic systems," *Tech. Rep. REN-1038*, AQ:3 533 Oct. 2004.

[12] A. J. Collin, "Advanced load modelling for power system studies," Ph.D. dissertation, School of Eng., The Univ. of Edinburgh, UK, 2014.

[13] S. Djokic, R. Langella, J. Meyer, R. Stiegler, A. Testa and X. Xu, "On evaluation of power electronic devices' efficiency for nonsinusoidal voltage supply and different operating powers," *IEEE Trans. Instrum. Meas.*, vol. 66, no. 9, pp. 2216-2224, Sep. 2017.

[14] R. Langella, A. Testa, J. Meyer, F. Möller, R. Stiegler and S. Z. Djokic, "Experimental-Based evaluation of PV inverter harmonic and interharmonic distortion due to different operating conditions," *IEEE Trans. Instrum. Meas.*, vol. 65, no. 10, pp. 2221-2233, Oct. 2016.

[15] X. Xu, S. Djokic, R. Langella and A. Testa, "Impact of lost periodicity on efficiency and current waveform distortion of SMPS'," *in Proc. 2017 IEEE Int. Workshop on Applied Meas. for Power Systems*, Liverpool, United Kingdom, pp. 1-6, Sept. 2017.

[16] L. Alfieri, A Bracale and G Carpinelli, "New ESPRIT-based method for an efficient assessment of waveform distortions in power systems," *Electric Power Systems Research*, vol. 122, pp. 130-139, May 2015.

[17] M. Biswal and P. K. Dash, "Estimation of time-varying power quality indices with an adaptive window-based fast generalised S-transform," *IET Sc., Meas. Tech.*, vol. 6, no. 4, pp. 189-197, Jul. 2012.

[18] K. Thirumala, A. Umarikar and T. Jain, "Estimation of single-phase and three-phase PQ indices using empirical wavelet transform," *IEEE Trans. Power Del.*, vol. 30, no. 1, pp. 445-454, Feb. 2015.

[19] M. Brey, "Review of computer energy consumption and potential savings", DSS Report, Dec. 2006.

[20] Dell Client Energy Savings Calculator [Online], Available: http://www.dell.com/downloads/global/products/optix/en/dell-client-energy-calculator-en.pdf

[21] *Electromagnetic Compatibility (EMC) – Part 4-30: Testing and measurement techniques-General guide on harmonics and interharmonics measurements and instrumentation, for power supply systems and equipment connected thereto*, IEC Std 61000-4-30, 2008.

[22] *IEEE Standard Definitions for the Measurement of Electric Power Quantities under Sinusoidal, Non-Sinusoidal, Balanced, or Unbalanced Conditions*, IEEE Std 1459-2010, 2010.

[23] TA041 Differential Probe Specification [Online], Available: http://www.farnell.com/datasheets/1694211.pdf

[24] LEM PR50 oscilloscope probe [Online], Available: http://docs-europe.electrocomponents.com/webdocs/0238/0900766b80238ae6.pdf

[25] HZO50 current Probe [Online], Available: http://www.testequipmentdepot.com/hameg/pdf/hz050_man.pdf

[26] SIRIUS Technical Reference Manual [Online], Available: https://www.dewesoft.com/download?file=SIRIUS_TechnicalReferenceManualV1.5.0.pdf